

# Role of the Alkyl Moiety and Counter Ions on the Thermal Stability of Chitosan Derivatives

Douglas de Britto,<sup>1</sup> Sergio Paulo Campana Filho,<sup>2</sup> Odilio B. G. Assis<sup>1</sup>

<sup>1</sup>Embrapa Instrumentação Agropecuária, Rua XV de Novembro, 1452, C.P. 741, São Carlos, SP 13560-970, Brazil

<sup>2</sup>Instituto de Química de São Carlos, Av. Trabalhador São-carlense, 400, C.P. 780, São Carlos, SP 13560-970, Brazil

Received 1 June 2010; accepted 7 October 2010

DOI 10.1002/app.33545

Published online 24 February 2011 in Wiley Online Library (wileyonlinelibrary.com).

**ABSTRACT:** The thermal stability of alkyl chitosan derivatives (RChi) and *N,N,N*-trimethyl chitosan bearing different counter ions (TMCX) was assessed by means of TG analyses. Multistep TG curves were observed for TMCX regardless of the counter ion. They exhibited lower DTG peak temperatures (TMCCI/238.2°C, TMCBBr/224.5°C, TMCI/222.6°C, and TMC-SO<sub>4</sub>/237.0°C) as compared to the parent chitosan (306.4°C) while, in contrast, the RChi showed higher DTG temperatures (ButChi/311.7°C, OctChi/327.8°C,

and DodecChi/306.3°C). The apparent activation energy values determined by using the isoconversional method revealed that the RChi derivatives have low activation energy (OctChi/111.6 ± 5 kJ/mol), whereas quaternary salts have high activation energy (TMCI/155.5 ± 10 kJ/mol). © 2011 Wiley Periodicals, Inc. *J Appl Polym Sci* 121: 815–822, 2011

**Key words:** thermal degradation; *N,N,N*-trimethyl chitosan; *N*-alkyl chitosan; isoconversional kinetic

## INTRODUCTION

The *N*-methylation of chitosan allows the preparation of *N,N,N*-trimethyl chitosan (TMC), a reaction which may be carried out by reacting chitosan with excess of iodomethane in suspension of *N*-methyl-2-pyrrolidone<sup>1</sup> or by the dimethylsulfate's synthetic route.<sup>2</sup> Such derivatization is very interesting because it results in samples with improved solubility since the chitosan itself is soluble only in moderately acidic aqueous solutions due to the reversible protonation of its amino sites, while TMC is soluble over a wide pH range. These derivatives have found several applications in recent experiments as gene delivery tools<sup>3,4</sup>; absorption enhancers for hydrophilic drugs across intestinal epithelia<sup>5,6</sup>; antibacterial agent showing higher activity than chitosan<sup>7,8</sup> as nanoparticles for vaccines<sup>9</sup>; and in controlled drug release.<sup>10</sup> Furthermore, being bactericidal and fungicidal<sup>11,12</sup> and able to form films easily<sup>13</sup> as well as possessing properties such as biodegradability and nontoxicity make these derivatives potential materials for use in natural products.<sup>14</sup>

The TMC can be prepared in different salts forms by simply exchanging its counter ions, though the

chloride form is preferred due to its stability in the solid state, easiness of isolation and nontoxicity. In fact, for any polyelectrolyte, the counter ion exchanging provokes changes in its physical chemistry properties such as the polymer solubility, the hydrophilic/hydrophobic balance, density, and morphology. Chitosan itself can also be prepared in different salt forms exhibiting distinct properties. Indeed, some studies carried out on chitosan salts have reported different mechanical properties<sup>15</sup>; differences in drug release, swelling, erosion, and mucoadhesiveness profile<sup>16,17</sup> as well as playing important role in drug–polymer and excipient–polymer interactions<sup>18</sup> as a function of the chitosan-associated counter ion. However, no reports have been found relating the properties of TMC salt with the counter ion nature. In this way, the study of TCM in different salts forms is important both to provide a best comprehension of its cationic nature as well as allowing to improve its processability and broaden its range of applications.<sup>6</sup> In fact, the already well-known properties of TMC, as quoted earlier, could be markedly improved by only exchanging the counter ions.

The thermal degradation kinetics of TMCCI was studied in a previous work, showing that the polymer stability depends on its average degree of quaternization, for which the higher the content of trimethylated ammonium sites, the lower was the thermal stability of TMCCI.<sup>1</sup> Accordingly, the apparent activation energy of the thermal degradation was lower as the higher was the average degree of quaternization of TMCCI.

Correspondence to: D. de Britto (britto@cnpdia.embrapa.br).

Contract grant sponsors: FAPESP, CNPq, EMBRAPA.

In this study, the influence of different counter ions (TMCX) and of the length of alkyl substituents (RChi) on the thermal stability of chitosan derivative was evaluated by TG analyses.

## EXPERIMENTAL

### Synthesis of the alkyl derivatives and quaternary salts

Chitosan of medium molecular weight (Brookfield viscosity 200 cP) was purchased from Sigma-Aldrich Corp. (St. Louis, MO) and was used for the preparation of chitosan derivatives. Dimethylsulfate was obtained from Vetec (R. Janeiro, Brazil) and the other chemicals were supplied by Synth (S. Paulo, Brazil). NaI, NaBr, NaCl, NaF, CH<sub>3</sub>COONa, and Na<sub>2</sub>SO<sub>4</sub>, all of chemical grade, were purchased from Mallinckrodt, Carlo Erba, and Aldrich.

The alkylation of chitosan was achieved by reacting the polymer with appropriated aldehyde followed by reduction with sodium cyanohydroxide.<sup>14,19</sup> The use of the molar ratios 2 : 1 butyraldehyde:chitosan, 0.5 : 1 octylaldehyde : chitosan, and 0.1 : 1 dodecyl aldehyde : chitosan resulted in *N*-butylchitosan, *N*-octylchitosan, and *N*-dodecylchitosan derivatives named as ButChi, OctChi, and DodecChi, respectively.

The reaction aiming the preparation of quaternary salts was carried out according to the procedure described by Britto and Assis.<sup>2</sup> Thus, 1 g of sample (chitosan or its alkyl derivatives) were suspended in 20 mL of dimethylsulfate/deionized water (4/1 v/v), 1.2 g of NaOH (0.015 mol) and 0.88 g of NaCl (0.015 mol). This suspension was stirred for 6 h by means of a magnetic stirring at room temperature. The final product was isolated after dialysis against water and NaCl 0.1 M, neutralized with 0.1 M aqueous NaOH and precipitated upon addition of acetone. This procedure yielded the quaternary salts *N,N,N*-trimethylchitosan (TMC), *N*-butyl-*N,N*-dimethylchitosan (ButDMC), *N*-octyl-*N,N*-dimethylchitosan (OctDMC), and *N*-dodecyl-*N,N*-dimethylchitosan (DodecDMC).

### TMCX salts in different counter ions forms

To obtain TMC in different salts forms, an aqueous solution (Cp = 1%) was submitted to dialysis (cellophane membrane from Aldrich; cut-off 12,000–14,000 g mol<sup>-1</sup>) for 3 days against 0.1 M aqueous NaX, (X = I, Br, Cl, F, CH<sub>3</sub>COO, SO<sub>4</sub>). The TMCX salts forms (iodide, bromide, chloride, fluoride, acetate, and sulfate) were precipitated by adding acetone to the dispersion, followed by exhaustive washing and drying at room temperature.

### Characterizations

The parent chitosan and its derivatives were characterized by infrared (FTIR), <sup>1</sup>H-nuclear magnetic reso-

nance (<sup>1</sup>H-NMR), and solid-state <sup>13</sup>C-nuclear magnetic resonance (CP-MAS <sup>13</sup>C-NMR) spectroscopies, as published before.<sup>2,14,20</sup> Briefly, they were: thin films ( $\theta \approx 0.1$  mm) prepared by casting for FTIR analyses which were carried out in a Perkin-Elmer spectrometer (model Paragon 1000); the <sup>1</sup>H-NMR spectra were acquired at 353 K by using a 200 MHz spectrometer (Bruker AC200). Chitosan and TMC salts were dissolved in D<sub>2</sub>O/HCl (100/1 v/v) and in D<sub>2</sub>O, respectively, at a concentration of 10 mg mL<sup>-1</sup>; the solid-state CP-MAS <sup>13</sup>C-NMR experiments were performed on a Varian Unity Inova 400 spectrometer operating at 400 MHz for <sup>1</sup>H frequency, using the combined techniques of proton dipolar decoupling (DD), magic angle spinning (MAS), and cross-polarization (CP). Contact time was 1 ms, acquisition time 51.2 ms, and the recycle delay 4 s. The proton pulse width was 6 ms, and an 18 kHz spectral window was used. Typically 2000 scans were acquired for each spectrum.

Energy dispersive X-rays (EDX) spectroscopy analyses were conducted in a 440 Zeiss-Leika Scanning Electronic Microscopy (SEM) equipment, equipped with a silicon-lithium detector window (7060 Oxford EDX) with a resolution of 133 eV. The intensity of applied bundle of electrons was 20 keV. The analysis was performed in four different points of the surface sample.

### Thermal analysis and kinetic study

The samples were milled in a blender and sieved through a 125- $\mu$ m mesh sieve. After this, the samples were conditioned for 1 week at anhydrous atmosphere. The dynamic and isothermal degradation studies were carried out using 7 mg of sample under nitrogen atmosphere (gas flow of 60 mL min<sup>-1</sup>) in a TGA500 from TA Instruments.

For the dynamic experiments, the samples were heated from room temperature to 500°C at three different heating rates (5.0, 10.0, and 15.0°C min<sup>-1</sup>). For the isothermal experiments, the samples were heated at 10°C min<sup>-1</sup> to 150°C, maintained at this temperature for 10 min and then equilibrated at the desired temperature for more 80 min.

Different approaches<sup>1,21</sup> were applied to the isothermal and dynamic data aiming at evaluating the kinetic parameters and its effectiveness in modeling the thermal stability of chitosan and derivatives.

## RESULTS AND DISCUSSION

The amino groups of the 2-amino-2-deoxy-D-glucopyranose units in chitosan chain are the reactive sites where the alkylation and quaternization reactions occur (Fig. 1). Therefore, the reaction proceeds via electrophilic substitution of nitrogen. This

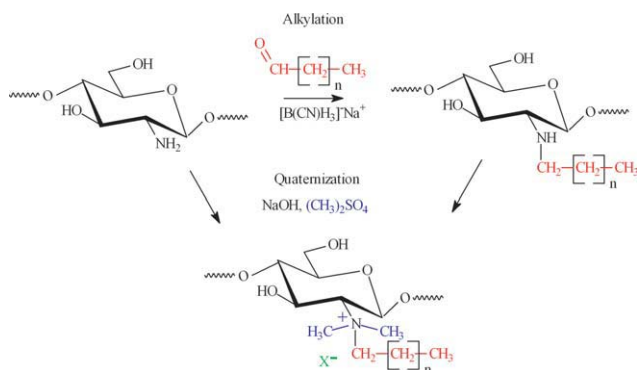


**Figure 1** Schematic representation of chitosan alkylation and quaternization. [Color figure can be viewed in the online issue, which is available at [wileyonlinelibrary.com](http://www.interscience.wiley.com).]

synthetic route also yields undesirable *O*-methylated products. The spectral characterization proves the structural changes after these reactions.

### Spectral characterization

The FTIR spectroscopy confirmed the occurrence of methylation of chitosan<sup>20</sup> and the presence of the counter ion acetate in the case of sample TMCac, as following:  $\nu_{max}/cm^{-1}$ : (a) 1475s (asymmetric bending

of C—H in CH<sub>3</sub> groups), present in the spectra of TMCi, TMCBr, and TMCac but absent in the spectrum of chitosan; (b) 1577s (bending of N—H) present in the chitosan spectrum but weak and shifted (1559) in the spectra of TMCi and TMCBr; and (c) 1568vs (stretching of C=O) and 1404s (asymmetric stretching of C—O) due to the acetate counter ion in the TMCac spectrum.

The <sup>1</sup>H-NMR spectroscopy also confirmed the evidences of the methylation,<sup>2,14,20</sup> as following,  $\delta_H$  (200 MHz, D<sub>2</sub>O): 4.5–5.5 (1-H of the glycosidic ring, w br); 4.1 (H, residual H<sub>2</sub>O); 3.37, 3.56 (3 H, s, CH<sub>3</sub> in *O*-methylated hydroxyl sites); 3.27 (9 H, versus, CH<sub>3</sub> in *N,N,N*-trimethylated amino site); 2.76 (6 H, s, CH<sub>3</sub> in *N,N*-dimethylated amino site); 2.01 (3 H, s, CH<sub>3</sub> in chitosan acetamide moiety); 1.85 (3 H, versus, CH<sub>3</sub>COO<sup>-</sup>, exceptionally for TMCac spectrum).

Evidences of chitosan methylation by CP-MAS <sup>13</sup>C-NMR spectroscopy were as follows,<sup>14,20</sup>  $\delta_C$ (400 MHz, solid state, externally referenced HMB at 17.3): 68.5 (1 C, merged with C-3 and C-5 of the glycosidic ring, CH<sub>3</sub> in *O*-methylated hydroxyl sites); 56.4 (3 C, merged with C-2 and C-6 of the glycosidic ring, CH<sub>3</sub> in *N,N,N*-trimethylated amino site); 48.1 (2 C, m, CH<sub>3</sub> in *N,N*-dimethylated amino site); 37.9 (1 C, m,

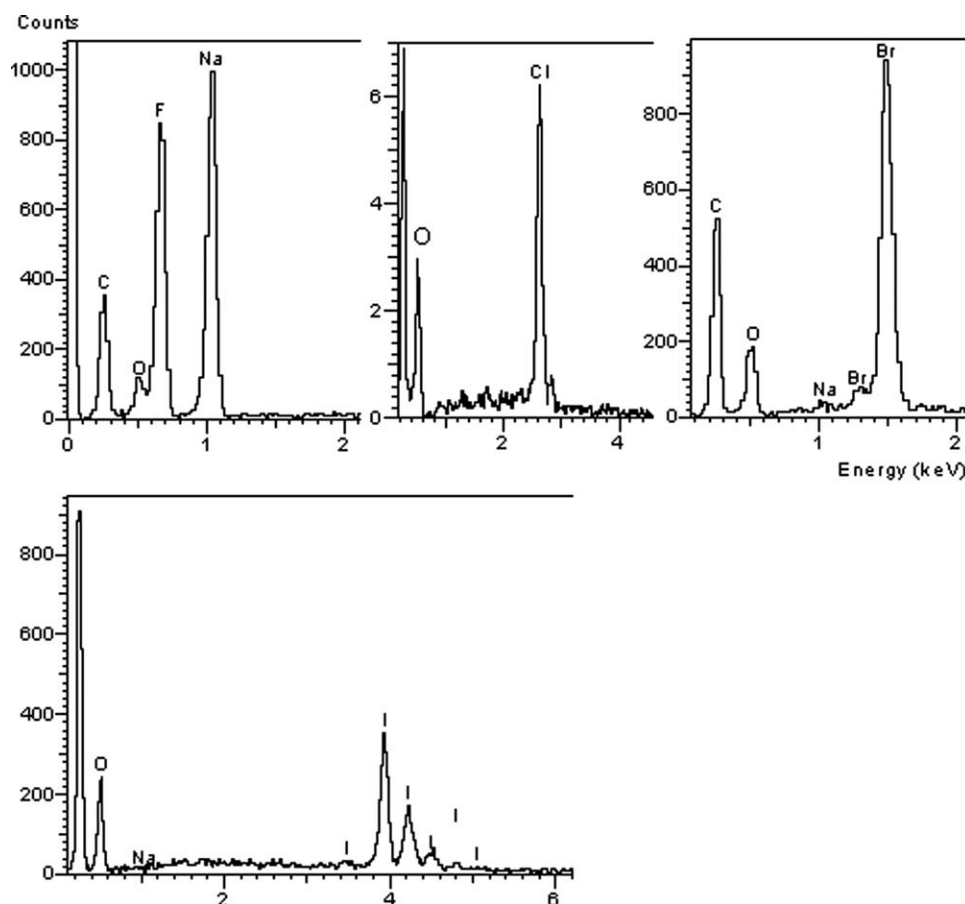


**Figure 2** Typical EDX spectra for TMC in different counter ion forms.

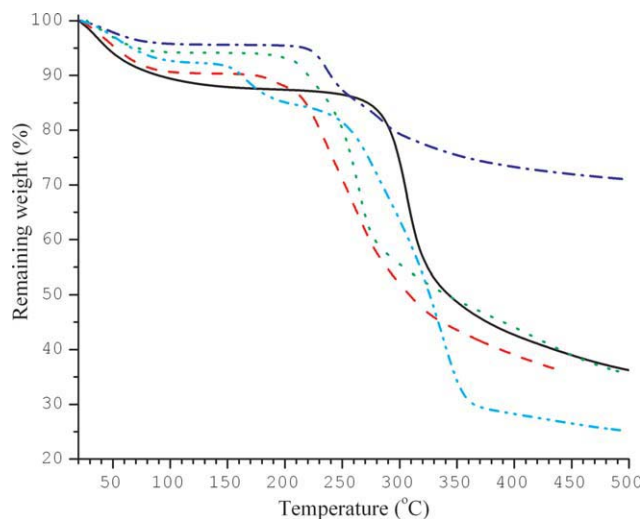


**Figure 3** Typical TG curves of TMC in the range 25–500°C, in  $N_2$  atmosphere, scanned at heating rate,  $\beta = 10^\circ C \text{ min}^{-1}$ , for the following samples: chitosan (—); TMCCl (---); TMCI (.....);  $TMCSO_4$  (-.-.-); and TMCAC (— · — ·). [Color figure can be viewed in the online issue, which is available at [wileyonlinelibrary.com](http://wileyonlinelibrary.com).]

$CH_3$  in *N*-monomethylated amino site); 25.8 (1 C, overlapped,  $CH_3COO^-$ , exceptionally for TMCAC spectrum); 24.3 (1 C, overlapped,  $CH_3$  in chitosan acetamide moiety). The degree of quaternization determined by this technique<sup>20</sup> was 40.04%.

The EDX spectroscopy is a valuable tool to elucidate the nature of the counter ions of TMC salts and to verify the purity of the sample. Figure 2 shows typical EDX spectra of TMC salts, allowing the observation of the signals generated by the counter ion. As reported in the literature,<sup>22</sup> the main X-ray properties for edge energies in keV are  $K\alpha = 1.04$  for Na;  $K\alpha = 0.69$  for F;  $K\alpha = 2.62$ ,  $K\beta = 2.82$  for Cl;  $L\alpha = 1.48$ ,  $L\beta = 1.53$  for Br; and  $L\alpha = 3.94$ ,  $L\beta = 4.22$  for I. It is worth noticing that all of the X-rays lines from the EDX spectra of TMC salts (Fig. 2) match very well with those reported in the literature. Moreover, only a small signal at 1.02 keV, which is referent the presence of sodium salt in the samples, is observed in the spectra of TMCAC and  $TMCSO_4$ .

The solubility of the inorganic salts determines the easiness in obtaining TMC free from coprecipitated salt. From Figure 2, it is noticeable that a huge contamination of the TMCF sample by NaF due to the low solubility of this inorganic salt. Indeed, the solubilities of the salts used in the dialyzes are as follows<sup>23</sup>: NaF: (wt = 4.22 g/cm<sup>3</sup>; et = very slightly soluble); NaCl: (wt = 35.7 g/cm<sup>3</sup>; et = slightly soluble); NaBr: (wt = 116 g/cm<sup>3</sup>; et = slightly soluble); NaI: (wt = 184 g/cm<sup>3</sup>, et = 42.57 g/cm<sup>3</sup>);  $Na_2SO_4$ : (wt = soluble); and  $NaCH_3COO$ : (wt = 119 g/cm<sup>3</sup>; et = slightly soluble), where “wt” and “et” stand for the solubility in water and ethanol, respectively. According to these data and considering only

the isolation process, the last four salts are more convenient due to its good solubility, avoiding the coprecipitation phenomenon.

### Thermal stability

The TG curves of chitosan and its derivatives acquired at heating rate of  $10^\circ C \text{ min}^{-1}$ , from room temperature to 500°C, are shown in Figure 3. The first thermal event in the range 25–140°C is attributed to water evaporation which is affected by the nature of the counter ion. For the salts  $TMCSO_4$ , TMCI, TMCBr, TMCAC, and TMCCl, conditioned in anhydrous atmosphere, the losses of weight due to the evaporation of water corresponded to:  $4.4 \pm 0.2$ ;  $6.1 \pm 0.4$ ;  $7.1 \pm 0.7$ ;  $8.2 \pm 0.7$ , and  $9.1 \pm 0.7$ , in %. Thus, the salt  $TMCSO_4$  seems to be the most appropriate form to be stored for a long time because of its low water affinity. In contrast, the samples TMCI, TMCBr, TMCAC, and TMCCl absorb water from the ambient humidity indefinitely, becoming eventually a gel like material. This knowledge is very important, for example, for use in pharmaceutical formulations (excipient vehicle in tablet, beads, etc) as a release-controlling agent in oral preparations,<sup>24</sup> once the three-dimensional stability relies on electrostatic, hydrophobic, and/or hydrogen bonding forces between the polymeric chains rather than chemical bonds.

The thermal event occurring in the range 140–400°C is attributed to the chain polymeric degradation. The chitosan pyrolysis is an extremely complex process,<sup>25,26</sup> generally involving a series of reactions. This complexity is highlighted by the multipieaks pattern observed in the derivative of the TG curves (DTG) of TMC samples (Fig. 4). In an attempt to understand this behavior, the peaks were grouped according to its proximity in terms of

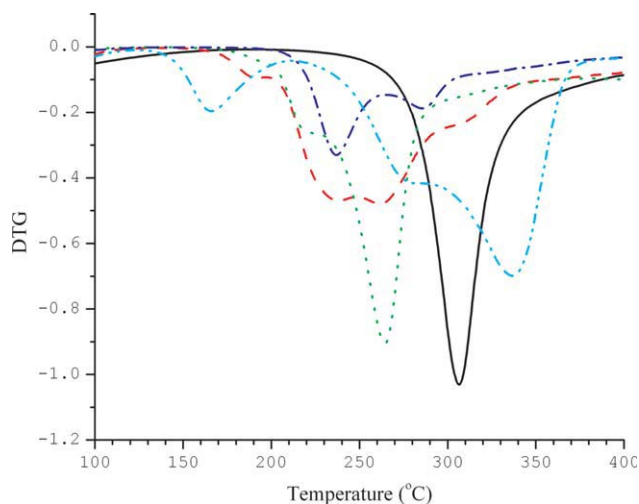


**Figure 4** Corresponding DTG curves for TG curves showed in the Figure 2. [Color figure can be viewed in the online issue, which is available at [wileyonlinelibrary.com](http://wileyonlinelibrary.com).]



**TABLE I**  
**Characteristics Peak Temperatures, in °C, for the DTG Curves (from Fig. 3); Onset Point, in °C, and Weight Loss, in %, (from Fig. 2) in the Range 140–400°C**

Sample	Onset	Peak A	Peak B	Peak C	Peak D	Weight loss
Chitosan	288.7	–	–	–	306.4	46.4
TMCF	209.6	–	239.2	–	306.9	46.4
TMCCI	211.0	192.3	238.2	262.2	313.7	46.9
TMCCI <sub>acd</sub>	211.8	–	224.9	–	–	39.4
TMCBr	235.4	194.7	224.5	261.8	–	40.8
TMCI	237.7	193.2	222.6	264.4	–	46.1
TMCSO <sub>4</sub>	223.5	–	237.0	285.6	–	21.2
TMCAc	152.4	166.3	–	285.0	336.5	63.8
ButChi	286.1	–	–	–	311.7	73.87
ButDMC	236.8	–	–	265.2	308.1	72.5
OctChi	300.1	–	–	–	327.8	81.6
OctDMC	231.3	–	–	250.0	–	45.1
DodecChi	290.7	–	–	–	306.3	50.6
DodecDMC	244.2	–	–	268.3	–	46.7

temperature but they do not reflect necessarily the same thermal reaction. The results of this analysis as well as the weight losses occurring in this range of temperature are resumed in Table I. Considering the aforementioned data, the main difference between chitosan and TMCX is that the former shows a single peak<sup>21</sup> while the last show more than one. It is clear that other kind of chain degradation takes place for TMCX salts. Moreover, the first DTG peak regarding the TMCX samples and the onset point occur with no exception, at lower temperatures as compared to the parent chitosan.<sup>1</sup> This is an important fact, allowing one to conclude that the quaternary salts are less thermally stable in relation the degradation onset.

Analyzing the Table I, the peak assigned as “A” seems to correspond to the same degradation reaction for TMCCI, TMCBr, and TMCI once its shape and position are quite similar for these samples, while for TMCAc it occurs at a much lower temperature (Table I). Although very different from others TMC degradation pattern, it is not possible yet to assure whether the peak “A” corresponds to the degradation of the acetate counter ion itself or if its presence induced the occurrence of a by-degradation reaction. The next peak, named “B,” is more intense than peak “A” and the temperatures where it occurs allow the establishment of a sequence of increasing thermal stability as TMCI  $\approx$  TMCBr < TMCCI  $\approx$  TMCF  $\approx$  TMCSO<sub>4</sub>. On the other hand, according to onset point values (Table I) the sequence of increasing thermal stability would be TMCAc < TMCF < TMCCI < TMCSO<sub>4</sub> < TMCBr < TMCI. This last sequence looks to be more reliable once it is in good agreement with the sequence of activation energy, discussed below. In a way, for the counter ions pertaining to the halogen family, the stability of TMCX seems to be linked to ionic radius of the halide (2.2, 1.96, 1.81, and 1.33 Å for I<sup>−</sup>, Br<sup>−</sup>, Cl<sup>−</sup>, and F<sup>−</sup>, respectively). The last two peaks observed in the

DTG curves for the chitosan derivatives correspond to further stages of the degradation of the polymers as well as to the degradation of those species formed in the previous steps. The complex set of simultaneous reaction occurring above 400°C prevents the proposition of any comparison between the samples.

It is known that the pH plays an important role on the physical chemistry properties of cationic polyelectrolyte-like chitosan<sup>27</sup> and TMC salts. Particularly for TMC applications, caution must be taken once TMC recovered from an acid medium, say aqueous hydrochloric acid, is predominantly a chitosan hydrochloride. Thus, in addition to its quaternary sites, the TMC has acid sites from which protons can dissociate, a factor which may affect the polymer properties, including its thermal stability. As shown in Figure 5 and according to the data in Table I, the sample TMCCI<sub>acd</sub>, which was recovered from aqueous hydrochloric acid, is less stable than the sample TMCCI, which was recovered from a neutral medium, as the onset temperature for its thermal degradation is lower as compared to TMCCI.

The alkyl derivatives of chitosan showed DTG peak and onset point values at temperature considerable higher than that of the parent chitosan (Fig. 6 and Table I), the highest value corresponding to OctChi. It is a new and interesting fact once, generally, chitosan derivatives show lower thermal stability than chitosan itself, as reported for Schiff bases<sup>28</sup>; cyclic oxygenated<sup>29</sup>; lactic/glycolic sided chain<sup>30</sup>; and mercaptan<sup>31</sup> derivatives of chitosan. Also, chitosan metal complex showed similar trend.<sup>32</sup> The possible reasons for such behavior are still unclear, but it can be attributed to hydrophobic interactions which could confer some additional stability to the bulk polymer. On the other hand, the quaternization of chitosan is really detrimental to the thermal stability of the polymer as evidenced in the TG and DTG curves for quaternary salts of alkyl

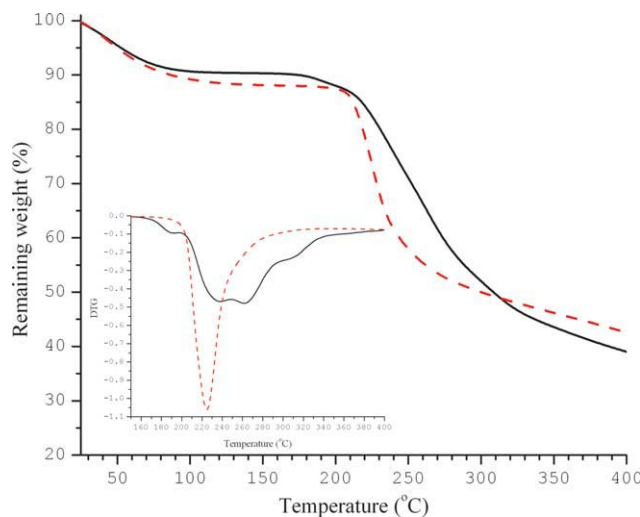


**Figure 5** TG curves for TMCCl (—) and TMCCl<sub>acd</sub> (---) in the range 25–400°C, in N<sub>2</sub> atmosphere, scanned at heating rate,  $\beta = 10^\circ\text{C min}^{-1}$ . Insert: Corresponding DTG curves for the range 150–400°C. [Color figure can be viewed in the online issue, which is available at [wileyonlinelibrary.com](http://wileyonlinelibrary.com).]

chitosan derivatives (Fig. 6). In all cases, the DTG peaks for the correspondent quaternary salt ButDMC; OctDMC and DodecDMC shifted to lower temperatures values (Table I). On the other hand, these alkyl chitosan quaternary salts showed improved thermal stability in comparison with trimethylated salts (TMCX). It is a very important feature mainly for food<sup>14</sup> and packaging<sup>33</sup> destination, for preparation of edible coating film and skin protection, for example.

The kinetics of the thermal degradation of polymers can be evaluated from the TG curves by using adequate mathematical modeling, allowing the determination of the apparent activation energy,  $E_a$ , the frequency factor,  $A$ , and the kinetic model,  $f(\alpha)$ .<sup>1,21</sup> Previous studies<sup>21,30</sup> have revealed that the thermal degradation of chitosan exhibits a clear trend of increasing  $E_a$  with increasing extent of conversion,  $\alpha$ , suggesting the occurrence of complex reactions at the latter stages of degradation. On the other hand, the thermal degradation curves for TMC salts present multiples steps and modeling the degradation kinetics is a very complex task.

A general equation that correlates the three main kinetic parameters of a thermal degradation process is expressed by:

$$\frac{d\alpha}{dt} = k(T)f(\alpha) \quad (1)$$

where  $t$  is the time,  $\alpha$  is the extent of reaction,  $T$  is the temperature,  $k(T)$  is the temperature-dependent

rate constant, and  $f(\alpha)$  is a temperature-independent function that represents the reaction model. The rate constant  $k(T)$  is given, generally, by the Arrhenius equation:

$$k(T) = A \exp\left(-\frac{E_a}{RT}\right) \quad (2)$$

where  $A$  is the pre-exponential or frequency factor, and  $E_a$  is the apparent activation energy. Thus, eq. (1) may be rewritten as:

$$\frac{d\alpha}{dt} = A \exp\left(-\frac{E_a}{RT}\right)f(\alpha) \quad (3)$$

If the temperature is changed with the time ( $\beta = dT/dt$ ) as it occurs in dynamic experiments, eq. (3) assumes the form:

$$\frac{d\alpha}{dt} = \frac{A}{\beta} \exp\left(-\frac{E_a}{RT}\right)f(\alpha) \quad (4)$$

which, by integration results in:

$$g(\alpha) = \frac{A}{\beta} \int_0^T \exp\left(-\frac{E_a}{RT}\right) dT = \frac{A}{\beta} I(E_a, T) \quad (5)$$

where  $g(\alpha)$  results from the integration of  $f(\alpha)$ .

Several methodologies and mathematical approaches have been proposed<sup>34</sup> to solve eq. (5) and to determine  $E_a$ , as the isoconversational method

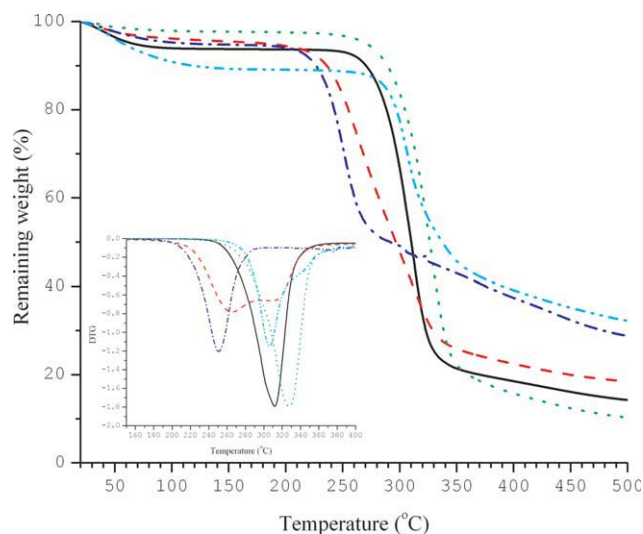


**Figure 6** TG curves for ButChi (—); ButDMC (---); OctChi (.....); OctDMC (-.-.-); and DodecChi (— · —) in the range 25–400°C, in N<sub>2</sub> atmosphere, scanned at heating rate,  $\beta = 10^\circ\text{C min}^{-1}$ . Insert: Corresponding DTG curves for the range 150–400°C. [Color figure can be viewed in the online issue, which is available at [wileyonlinelibrary.com](http://wileyonlinelibrary.com).]

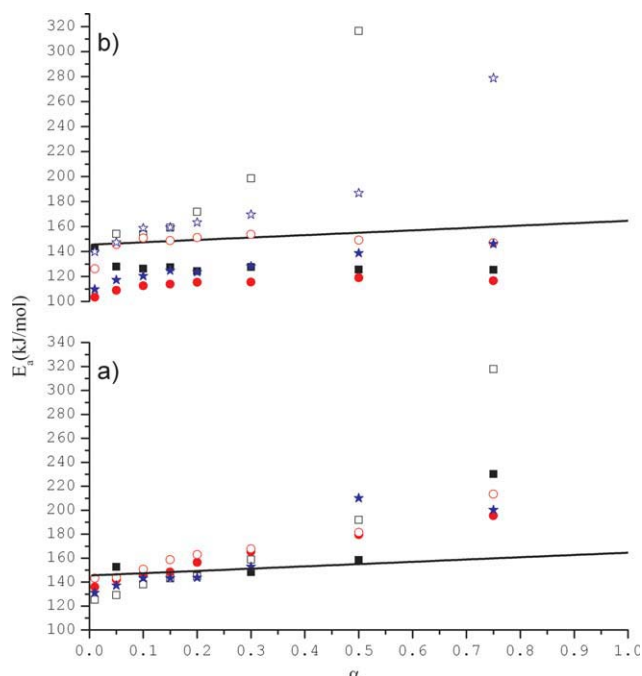


**Figure 7**  $E_a$  versus  $\alpha$  dependency calculated according to Ozawa-Flynn-Wall method for (a) TMC in different counter ion forms, with the following caption: chitosan (■); TMCCl (□); TMCBr (●); TMCI (○); TMCSO<sub>4</sub> (★) and for (b) alkyl derivatives, in which: ButChi (■); ButDMC (□); OctChi (●); OctDMC (○); DodecChi (★); and DodecDMC (☆). The solid line corresponds to the linear fit for chitosan data in the range  $0.01 < \alpha < 0.4$ . [Color figure can be viewed in the online issue, which is available at [wileyonlinelibrary.com](http://wileyonlinelibrary.com).]

developed by Osawa-Flynn-Wall<sup>35</sup> that is claimed to be most reliable. This method uses the Doyle approximation<sup>36</sup> to solve the temperature integral [eq. (5)] and is expressed by:

$$\log \beta = \log \frac{AE_a}{g(\alpha)R} - 2.315 - \frac{0.4567 E_a}{RT} \quad (6)$$

Therefore, if a set of experiments is run at different heating rates,  $\beta$ , then the value of  $E_a$  can be obtained from the plot of  $\log \beta$  against  $1/T$  for a fixed degree of conversion,  $\alpha$ .

The plots of  $E_a$  versus  $\alpha$  for the thermal degradation of chitosan and TMC salts show the same trend of increasing  $E_a$  with increasing extent of conversion [Fig. 7(a)]. The values of  $E_a$  (kJ/mol) were calculated in the range  $0.01 < \alpha < 0.4$  and they correspond to: TMCCl/ $139.9 \pm 12 < \text{TMCSO}_4$ / $141.7 \pm 7 < \text{TMCBr}$ / $149.0 \pm 10 < \text{TMCI}$ / $155.5 \pm 10$ . As pointed earlier, this sequence is in good agreement with the sequence of increasing thermal stability regarding the onset point. It is an important find that, once chitosan quaternary salt is, generally, handled in its chloride form (TMCCl) but other counter ions forms has shown improved thermal

stability and interesting new properties. In this way, these new TMC kinds represent potential application in the industrial area.

In the field of thermal analysis, a different concept of activation energy that identifies the energy with the barrier to the bond redistribution processes was discussed before<sup>37</sup> although it is agreed that high value of  $E_a$  reflects in fast rate of thermal degradation. In this way, the trimethylation process increases the rate of thermal degradation of the derivative in comparison with parent polymer (chitosan/ $147.8 \pm 2$ ) except for the samples TMCCl and TMCSO<sub>4</sub>. In contrast, from the data expressed in Figure 7(b), the alkyl derivatives of chitosan presented lower  $E_a$  values (kJ/mol) than that chitosan: ButChi/ $126.5 \pm 1.3$ , OctChi/ $111.6 \pm 5$ , and DodecChi/ $120.7 \pm 7$ . In agreement with the TMCX data, the quaternary salts prepared from the chitosan alkyl derivatives showed high  $E_a$  values (kJ/mol): ButDMC/ $167 \pm 19$ , OctDMC/ $146.0 \pm 10$ , and DodecDMC/ $156.3 \pm 11$ . In conclusion, it is found that the *N*-alkylation of chitosan decreases the apparent activation energy (low degradation rate), while the extensive *N*-methylation, which generates positively charged sites on the polymer chains, increases the apparent activation energy (high degradation rate).

The kinetics of the thermal degradation of chitosan, TMCI, and TMCBr salts were further analyzed according to the isothermal method proposed by MacCallum.<sup>38</sup> For this, several isothermal experiments were carried out (insert in the Fig. 8), and the

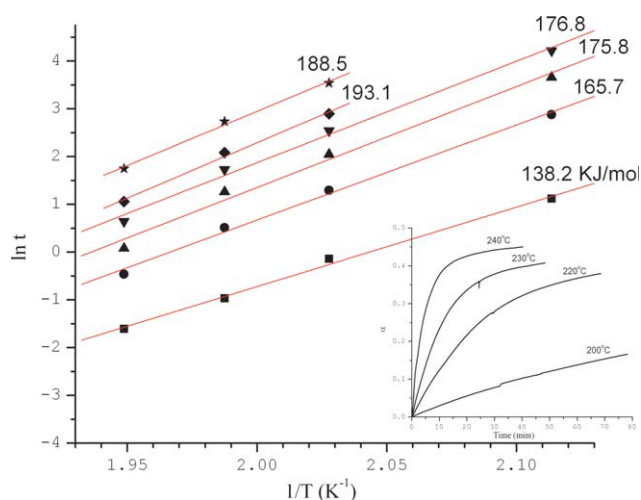


**Figure 8** Plots of  $\ln t$  versus  $1/T$  for the isothermal degradation of TMCI as a function of the extension of conversion:  $\alpha = 0.01$  (■);  $\alpha = 0.05$  (●);  $\alpha = 0.1$  (▲);  $\alpha = 0.15$  (▼);  $\alpha = 0.2$  (◆);  $\alpha = 0.3$  (★). Insert: Plots of  $\alpha$  versus reaction time for the isothermal degradation for TMCI at different temperatures. [Color figure can be viewed in the online issue, which is available at [wileyonlinelibrary.com](http://wileyonlinelibrary.com).]

experimental data were treated by using the following equation:

$$\frac{E_a}{RT} + \ln[g(\alpha)] - \ln A = \ln t \quad (7)$$

Thus, if the logarithm of the time,  $t$ , taken to reach a fixed extent of conversion,  $\alpha$ , is plotted against the reciprocal of the temperature then it will yield a straight line (Fig. 8) whose slope is  $E_a/R$ .

The curves corresponding to chitosan and TMCB<sub>r</sub> showed the same profile as that of sample TMCI (Fig. 8) and the average values of  $E_a$  (kJ/mol) determined in the range  $0.01 < \alpha < 0.4$  were as follows: chitosan/ $153.0 \pm 6.9$ , TMCI/ $184 \pm 21$ , and TMCB<sub>r</sub>/ $173 \pm 20$ . Such values confirm the same trend found above when the isoconversional method was applied, though resulting in higher values ( $\approx 19\%$ ) in the cases of the samples TMCI and TMCB<sub>r</sub>.

Concerning the kinetic model  $f(\alpha)$  which better describes the thermal degradation of the chitosan derivatives, the attempts made to fit the experimental data were unfruitful due to the multippeak pattern found in these cases when plotting  $da/dT$  versus  $\alpha$ . Thus, no single kinetic model is proposed in these cases, the occurrence of a complex set of consecutive reactions prevents such a proposition.

## CONCLUSIONS

The analyses of the DTG curves concerning the thermal behavior of quaternized chitosan salts and *N*-alkyl chitosan derivatives reveal that the thermal degradations of the former polymers begin at lower temperatures. The isoconversional method used as mathematical modeling to study the kinetics of the thermal degradation, showed that the *N*-alkyl chitosan derivatives has lower apparent activation energy than the quaternized chitosan salts. Thus, an important role is attributed to the presence of positively charged sites along the polymers chains in decreasing the thermal stability of these chitosan derivatives. TMC in different counter ion forms showed good thermal stability, except that having acetate ion as counter ion that was considerable less stable. A potential applied form can be TMCSO<sub>4</sub> that was very thermally stable with additional advantage to absorb less water.

## References

1. Britto, D.; Campana-Filho, S. P. *Polym Degrad Stab* 2004, 84, 353.
2. Britto, D.; Assis, O. B. G. *Carbohydr Polym* 2007, 69, 305.
3. Germershaus, O.; Mao, S. R.; Sitterberg, J.; Bakowsky, U.; Kissel, T. *J Controlled Release* 2008, 125, 145.
4. Sajomsang, W.; Ruktanonchai, U.; Gonil, P.; Mayen, V.; Opanasopit, P. *Carbohydr Polym* 2009, 78, 743.
5. Mourya, V. K.; Inamdar, N. N. *J Mater Sci: Mater Med* 2009, 20, 1057.
6. Sahni, J. K.; Chopra, S.; Ahmad, F. J.; Khar, R. K. *J Pharm Pharmacol* 2008, 60, 1111.
7. Kim, C. H.; Choi, J. W.; Chun, H. J.; Choi, K. S. *Polym Bul* 1997, 38, 387.
8. Jia, Z.; Shen, D.; Xu, W. *Carbohydr Res* 2001, 333, 1.
9. Amidi, M.; Romeijn, S. G.; Verhoef, J. C.; Junginger, H. E.; Bungener, L.; Huckriede, A.; Crommelin, D. J. A.; Jiskoot, W. *Vaccine* 2007, 25, 144.
10. Cafaggi, S.; Russo, E.; Stefani, R.; Leardi, R.; Caviglioli, G.; Parodi, B.; Bignardi, G.; De Toter, D.; Aiello, C.; Viale, M. *J Controlled Release* 2007, 121, 110.
11. Bautista-Baños, S.; Hernández-Lauzardo, A. N.; Velázquez-del Valle, M. G.; Hernández-López, M.; Barka, E. A.; Bosquez-Molina, E.; Wilson, C. L. *Crop Protection* 2006, 25, 108.
12. Rabea, E. I.; Badawy, M. E. T.; Stevens, C. V.; Smagghe, G.; Steurbaut, W. *Biomacromolecules* 2003, 4, 1457.
13. Hsu, S. H.; Whu, S. W.; Tsai, C. L.; Wu, Y. H.; Chen, H. W.; Hsieh, K. H. *J Polym Res* 2004, 11, 141.
14. Britto, D.; Assis, O. B. G. *Int J Biol Macromol* 2007, 41, 198.
15. Bégin, A.; Calsteren, M. R. V. *Int J Biol Macromol* 1999, 26, 63.
16. Cafaggi, S.; Leardi, R.; Parodi, B.; Caviglioli, G.; Russo, E.; Bignardi, G. *J Controlled Release* 2005, 102, 159.
17. Orienti, I.; Cerchiara, T.; Luppi, B.; Bigucci, F.; Zuccari, G.; Zecchi, V. *Int J Pharm* 2002, 238, 51.
18. Nunthanid, J.; Laungnatanan, M.; Sriamonsak, P.; Limmavapirat, S.; Puttipipatkachorn, S.; Lim, L. Y.; Khor, E. *J Control Release* 2004, 99, 15.
19. Desbrières, J.; Martinez, C.; Rinaudo, M. *Int J Biol Macromol* 1996, 19, 21.
20. Britto, D.; Forato, L. A.; Assis, O. B. G. *Carbohydr Polym* 2008, 74, 86.
21. Britto, D.; Campana-Filho, S. P. *Thermochim Acta* 2007, 465, 73.
22. McMaster, W. H.; Kerr Del Grande, N.; Mallett, J. H.; Hubbell, J. H. *Compilation of X-Ray Cross Sections; Lawrence Livermore National Laboratory Report: Argonne*, 1969.
23. Lide, D. R. *CRC Handbook of Chemistry and Physics*, 89th ed.; CRC Press: Boca Raton, 2009.
24. Hamman, J. H. *Marine Drugs* 2010, 8, 1305.
25. Wanjuna, T.; Cunxinb, W.; Donghua, C. *Polym Degrad Stab* 2005, 87, 389.
26. Bengisu, M.; Yilmaz, E. *Carbohydr Polym* 2002, 50, 165.
27. Holme, H. K.; Foros, H.; Pettersen, H.; Dornish, M.; Smidsrød, O. *Carbohydr Polym* 2001, 46, 287.
28. Tirkistani, F. A. A. *Polym Degrad Stab* 1998, 60, 67.
29. Tirkistani, F. A. A. *Polym Degrad Stab* 1998, 61, 161.
30. Qu, X.; Wirsén, A.; Albertsson, A.-C. *Polymer* 2000, 41, 4841.
31. Peniche-Covas, C.; Argüelles-Monal, W. M.; Román, J. S. *Polym Degrad Stab* 1993, 39, 21.
32. Taboada, E.; Cabrera, G.; Jimenez, R.; Cardenas, G. *J Appl Polym Sci* 2009, 2043, 114.
33. Britto, D.; Assis, O. B. G. *Packag Technol Sci* 2010, 23, 111.
34. Brown, M. E.; Maciejewski, M.; Vyazovkin, S.; Nomen, R.; Sempere, J.; Burnham, A.; Opfermann, J.; Strey, R.; Anderson, H. L.; Kemmler, A.; Keuleers, R.; Janssens, J.; Desseyn, H. O.; Li, C.-R.; Tang, T. B.; Roduit, B.; Malek, J.; Mitsunashi, T. *Thermochim Acta* 2000, 355, 125.
35. Ozawa, T. *J Therm Anal* 1970, 2, 301.
36. Doyle, C. D. *J Appl Polym Sci* 1962, 6, 639.
37. Galwey, A. K. *Thermochim Acta* 2003, 399, 1.
38. MacCallum, J. R. In *Comprehensive Polymer Science*; Booth, C.; Price C., Eds; Pergamon Press: Oxford, 1989; Vol. 1, p 903.